Available at: http://www.ictp.it/~pub_off IC/2006/065

United Nations Educational Scientific and Cultural Organization
and
International Atomic Energy Agency

THE ABDUS SALAM INTERNATIONAL CENTRE FOR THEORETICAL PHYSICS

CONVERSION OF OPTICAL WAVE POLARIZATIONS IN 1D FINITE ANISOTROPIC PHOTONIC CRYSTAL

N. Ouchani
Laboratoire de Dynamique et d'Optique des Matériaux, Département de Physique, Faculté des Sciences, Université Mohamed I, B.P. 524, 60000 Oujda, Morocco,

D. Bria[1]
Laboratoire de Dynamique et d'Optique des Matériaux, Département de Physique, Faculté des Sciences, Université Mohamed I, B.P. 524, 60000 Oujda, Morocco
and
The Abdus Salam International Centre for Theoretical Physics, Trieste, Italy,

A. Nougaoui and A. Daoudi
Laboratoire de Dynamique et d'Optique des Matériaux, Département de Physique, Faculté des Sciences, Université Mohamed I, B.P. 524, 60000 Oujda, Morocco.

Abstract

We show that by using one dimensional anisotropic photonic structures, it is possible to realize optical wave polarization conversion by transmission or by reflection. Thus a single incident S(P) polarized plane wave can produce a single reflected P(S) polarized wave and a single transmitted P(S) polarized wave. This polarization conversion property can be fulfilled with a simple finite superlattice constituted by anisotropic dielectric materials. We discuss the appropriate choices of the material and geometrical properties to realize such structures. The transmission and reflection coefficients are discussed in relation with the dispersion curves of the finite structure embedded between two isotropic substrates. Both transmission and reflection coefficients are calculated in the framework of Green's function method. The amplitude and the polarization characteristics of reflected and transmitted waves are determined as function of frequency ω, and wave vector $k_{//}$ (parallel to the interface) and the orientations of the principal axes of the layers constituting the SL. Moreover, this structure exhibits a coupling between S and P waves that does not exist in SL composed only of isotropic materials. Specific applications of these results are given for a superlattice consisting of alternating biaxial anisotropic layers $NaNO_2$/SbSi sandwiched between two identical semi-infinite isotropic media.

MIRAMARE – TRIESTE

July 2006

[1] bria@sciences.univ-oujda.ac.ma

1-Introduction

Crystal optical anisotropy plays a prominent role in many optoelectronic devices [1-9] such as modulators, integrated switches, interferometers, amplifiers, polarization splitters etc. Thus, it is important to control the polarization of light in order to obtain transverse-electric (TE)-transverse magnetic (TM) conversion. Hence several experiments [10, 11] and theoretical [12-15] works analyzed the mode conversion in film-waveguide magneto-optical systems. The desired combination of low loss and high conversion efficiency is very hard to obtain. In this work we propose a polarization converter using a one-dimensional finite anisotropic photonic crystal. Our converter exhibits a conversion of S (TE) $\Leftrightarrow$P (TM) in transmission and reflection, with an appropriate choice of the materials, geometry and special angle of incidence of light.

Different mathematical methods have been developed to study the scattering problems of plane electromagnetic waves. One of the most often used techniques for calculating the optical properties of a general anisotropic slab is the 4×4 transfer matrix method [16-30] developed by several authors and applied to a variety of anisotropic structures. The 4×4 matrix approach, formulated earlier by Berreman[31], is the most useful method to solve such problems because of its efficiency for any kind of anisotropy and number of layers. In recent works[32-35], some of authors have studied in detail the propagation of optical wave through one-dimensional, isotropic, periodic structure by using a Green's function approach[36-37]; in particular, they have focused on the tunneling of optical pulses through a finite superlattice(SL), and also derived the exact relation between the density of states and the phase times of the transmission or reflection coefficients in the case of scalar modes for any composite system sandwiched between two different homogeneous semi-infinite media, etc.

As compared to the anisotropic material, the propagation inside an isotropic material is easy to describe because S and P polarized waves remain uncoupled after transmission and reflection at an interface. However the Green's function formalism, developed previously for isotropic materials, can also be extended to the case of anisotropic materials. In this paper we give analytic expressions for reflection and transmission coefficients when an optical plane wave is incident towards a finite superlattice embedded between two semi-infinite isotropic media. The SL is formed out of a periodical repetition of two alternating birefringent biaxial layers in which their principal axes are oriented at arbitrary directions.

Our paper is organized as follows: in section II, we present our theoretical expressions of the reflection and transmission coefficients when either an S or P polarized wave is incident upon the interface separating the substrate and the superlattice. Section III shows the numerical results for a structure constituted by a finite SL made of $NaNO_2$/SbSI embedded between two semi-infinite isotropic media (air). The conclusion is presented in section IV.

2-Theory

The geometry studied in this paper is schematically depicted in figure 1. The finite SL is composed of alternating biaxial layers (1,2) within the unit cell n. It is embedded between two semi-infinite isotropic substrates. All the interfaces are taken to be parallel to the (XY) plane of a Cartesian (laboratory) coordinate system and the Z axis is parallel to the normal of the interfaces. The media forming the layers of the SL are assumed homogeneous, non magnetic and characterized by their diagonal dielectric tensor $\vec{\varepsilon}_D = diag(\varepsilon_x, \varepsilon_y, \varepsilon_z)$, where $\varepsilon_x, \varepsilon_y$ and ε_z are the dielectric constants in the corresponding principal axis system (x,y,z). For a given orientation of each crystal, its dielectric tensor is described by the Euler angles [38,39] θ, ϕ and ψ with respect to the fixed (XYZ) coordinates system. For the sake of simplicity and without loss of generality, we investigate in our present study, the effect of only the azimuth angle ϕ and omit the effect of the other two angles ($\theta = \psi = 0$). The axes of the birefringent layers are presented in figure 1.

In this paper, we study the optical waves in lamellar periodic structures in the framework of a Green function method called the interface response theory[36-37]. The object of this theory is to calculate the Green's function of a composite system containing a large number of interfaces that separate different homogenous media. The knowledge of this Green's function enables us to obtain different physical properties of the system such as the reflection and transmission coefficients of the waves. In this theory the Green's function of a composite system can be written as [37]:

$$g(DD)=G(DD)+G(DM)\left\{\left[G(MM)\right]^{-1}g(MM)\left[G(MM)\right]^{-1}-\left[G(MM)\right]^{-1}\right\}G(MD) \quad (1)$$

where D and M are respectively the whole space and the space of the interfaces in the lamellar system. G is a block-diagonal matrix in which each block G_i corresponds to the bulk Green's function of the subsystem i. All the matrix elements g(DD) of the composite material can be obtained from the knowledge of the matrix elements g(MM) of the g in the interface space M. The g(MM) is given by inverting the matrix g^{-1}(MM) formed out by a linear superposition of the surface matrix $g_S^{-1}(MM)$ of any independent film bounded by perfectly free interfaces with appropriate boundary conditions. The elements matrix $g_S^{-1}(MM)$ are given in the Appendix.

Within this theory, the reflected and transmitted waves u(D), resulting from a uniform plane wave U(D) incident upon a plane boundary between two different media, are given by [37]:

$$u(D)=U(D)+G(DM)\left\{\left[G(MM)\right]^{-1}g(MM)\left[G(MM)\right]^{-1}-\left[G(MM)\right]^{-1}\right\}U(M) \quad (2)$$

Let us mention that the incident wave, generated in the substrate S, can have two different polarizations, namely, transverse electric TE $(E \perp \text{plane of incidence})$ or magnetic TM (E // plane of incidence). Each wave propagating inside the anisotropic media generates two transmitted waves and two reflected waves with different polarizations. Let us call E_{iS} and $E_{i\,P}$

the amplitudes of the S and P components of the incident field. Then, the amplitudes of the reflected and transmitted fields can be written as

$$\vec{E}_{RS}(z) = r_{SS}\,\vec{E}_{i\,S}(z) + r_{SP}\,\vec{E}_{i\,P}(z) \tag{3}$$

$$\vec{E}_{TS}(z) = t_{SS}\,\vec{E}_{i\,S}(z) + t_{SP}\,\vec{E}_{i\,P}(z) \tag{4}$$

$$\vec{E}_{RP}(z) = r_{P\,S}\,\vec{E}_{i\,S}(z) + r_{P\,P}\,\vec{E}_{i\,P}(z) \tag{5}$$

$$\vec{E}_{TP}(z) = t_{P\,S}\,\vec{E}_{i\,S}(z) + t_{P\,P}\,\vec{E}_{i\,P}(z) \tag{6}$$

The expressions of r_{ij} and t_{ij} in these equations, with i,j=S or P, are given in the Appendix.

We note here that the total reflectivities for the P and S modes are:

$$R_P \equiv R_{P\,P} + R_{SP} = \left|r_{P\,P}\right|^2 + \left|r_{SP}\right|^2 \tag{7}$$

$$R_S \equiv R_{S\,S} + R_{PS} = \left|r_{S\,S}\right|^2 + \left|r_{PS}\right|^2 \tag{8}$$

and the total transmisson for the P and S modes have the following expessions:

$$T_P \equiv T_{P\,P} + T_{SP} = \left|t_{P\,P}\right|^2 + \left|t_{SP}\right|^2 \tag{9}$$

$$T_S \equiv T_{S\,S} + T_{PS} = \left|t_{S\,S}\right|^2 + \left|t_{PS}\right|^2 \tag{10}$$

3- Discussion and Numerical Results

In order to check the correctness of the derived expressions and demonstrate the interest of our approach, we consider a one-dimenional anisotropic periodic structure composed of six layers of birefringent biaxial material: $NaNO_2$ (i=1) and five layers of birefringent biaxial material: SbSI (i=2) with principal optical indices[32] $n_x^{(1)}$=1.344, $n_y^{(1)} = 1.411$, $n_z^{(1)} = 1.651$ and $n_x^{(2)} = 2.7$, $n_y^{(2)} = 3.2$, $n_z^{(2)} = 3.8$, respectively. The thicknesses d_1 and d_2 of the layers are chosen such that $n_z^{(1)} d_1 = n_z^{(2)} d_2$. The principal axes of the layers are oriented with azimuth angles ϕ_1 and ϕ_2 (with respect to the laboratory (X,Y) plane). The SL is embedded between two isotropic media (air). A simple example of such system is presented in figure 1. We show in figure 2 the reduced frequency versus the orientation ϕ_2 of the second crystal of the structure when the azimuthal angle ϕ_1 is taken to be zero. These modes are obtained from the maximum of transmission coefficients when the incoming light has a transverse magnetic (or P) polarisation. All the branches represent bulk modes induced by the multilayer structure. The number of branches corresponding to extended states in the SL increases with increasing the number N of periods, leading to the bulk bands of the infinite superlatice[40]. On the other hand, the position and the form of these branches change significantly versus the relative orientation of the principal axis of the two birefringent anisotropic layers constituting the SL as shown in figure (2-a,b and c). Figure 3 displays the behavior of these modes as a function of the incidence angles, showing slight modifications of the modes for different azimuthal rotation of SbSI layers with respect to $NaNO_2$ layers. After multiple reflection and

transmission in the anisotropic media constituting the superlattice, each single incident plane wave with S or P polarization produces two reflected and two transmitted waves that contain both S and P polarized optical waves. The transmision coefficients T_{PP} and T_{SP} at normal incidence are displayed in figure 4 versus the reduced frequency Ω, for different values of the azimuth angle ϕ_2. The T_{SP} is very low around 0° and 90° where S and P modes remain uncoupled. The situation is then similar to that corresponding to the cases of isotropic materials. On the other hand, in other directions, around 50°, the modes exhibit a full coupling of the S and P polarized optical waves, and reaches its maximum values T_{SP} = 0.9888 for $\phi_2 = 53°$. Let us recall that for any inhomogeneity in the multilayer structure, the same pictures are seen when a pure transverse electric wave is incident and the T_{PS}=T_{SP}. T_{PS} or T_{SP} is a measure of the converted mode amplitude and is determined primarily by a large magnitude of the off diagonal tensor element ε_{ij}. In this configuration the P polarized input light is converted with a polarization conversion efficiency of 98.88% to S polarized wave. The polarization conversion efficiency for S polarized input wave is equal to the P result. Figure 5 shows clearly the efficiency of polarization conversion as a function of the azimuthal angle ϕ_2. To further investigate the posibility of a complete mode conversion, we study in figure 6 the variation of the converted wave transmission T_{SP} versus the thickness d_{r1} of the last $NaNO_2$ layer (located in cell (N+1)) when keeping the thickness of the first layer of the SL equal to 2.01D. In this situation a high degree of polarization efficiency is achieved and reaches its maximum 99.12% for d_{r1}=14.01D. This inhomogeneity leads to a difference of T_{PS} and T_{SP} for TE and TM inputs. The conversion property is also obtained by reflection of P-wave at oblique incident angle $\theta = 15°$ but in the high frequency range, with an amplitude much lower than that found above in the case of the transmission conversion (see figure 7). The conversion of polarization occurs in the region when the coupling of S and P is very strong. In this case the high degree of conversion occurs at $\phi_2 = 54°$ with an reflection coefficient R_{SP} = 0.8164 (see figure 8). Accordingly, we have examined in figure 9 the change in polarization conversion efficiency as a function of the total number of layers (2N+1). It is shown that the amplitude of the converted field increases with increasing N, and becomes constant around N=54 reaching a value of 99.06%.

4-Conclusion

In summary we have demonstrated that a multilayer structure formed out two birefringent biaxial layers can be used to make polarization converters with appropriate choise of the incident angle, the frequency and the orientation of the axis. The polarization conversion is the result of the off-diagonal elements of the dielectric tensor that cause the coupling between modes of different types of polarization S and P. This process of conversion cannot be realized with an isotropic system. Moreover, to improve the conversion factor, we have proposed to add a buffer layer to the SL; this layer can be made with the same material as one of the constituents in the SL but with a different thickness. The presence of such

inhomogeneity in the system increases the degree of polarization efficiency for the input field but introduces a difference of the converted mode transmission T_{SP} or reflection $R_{SP,}$ when the incoming light is of P polarization, with respect to the converted mode transmission T_{PS} or reflection R_{PS} ,when the incoming light is of S polarization.

References

[1] I. Kiyat, A. Aydinli, and N.Dagli, IEEE Photon. Technol.Lett. 17(1), 100-102(2005)

[2] T. K.. Liang and H. k. Tsang, IEEE Photon. Technol.Lett.17(2),393-395(2005).

[3] E.Yablonovitch, J.Opt. Soc. Am. B., vol.10, No2, February1993.

[4] Y.-Q. Lu, Z.-L. Wan, Q. Wang, Y.-X. Xi and N.-B. Ming, APL 77(23), 3719(2000)

[5] A. Adibi, R. K. Lee,Y. Xu, A.Yariv, A. Scherer, Elecrtronic letters, vol.36, No,16August 2000

[6] M. Koshiba, Y. Tsuji, S. Sasaki, *« High-Performance Absorbing Boundary Conditions for Photonic Crystal Waveguide Simulations »*, IEEE Microwave and wireless components letters, vol. 11, No 4, April 2001.

[7] S. T. Chew, T. Itoh, *« PBG-Excited Split-Mode Resonator Bandpass Filter »*, IEEE Microwave and Wireless Components Letters, vol. 11, No 9, September 2001.

[8] I.C. Khoo and J.Ding, APL 81, 2496 (2002)

[9] A. D'Orazio, M. de Sario, V. Gadaleta, V. Petruzzelli, F. Prudenzano, *"Meander microstrip photonic bandgap filter using a Kaiser tapering window"*, Electronics Letters, vol. 37, No 19, 13th September 2001.

[10] Tien P K, Schinke D P and Blank S L 1974 Magneto-optics and motion of the magnetization in a film-waveguide optical switch J. Appl. Phys. 45 3059–68

[11] BrunsW K and Milton A F 1975 Mode conversion in planar-dielectric separating waveguides IEEEJ. Quantum Electron. 11 32–9

[12] D. I. Sementsov, A. M. Shutyi and O.V. Ivanov. Pure Appl. Opt. 4, 653-663 (1995).

[13] Gillies J R and Hlawiczka P 1976 TE and TM modes in gyrotropic waveguides J. Phys. D: Appl.Phys. 9 1315–22

[14] Hlawiczka P 1978 A gyrotropic waveguide with dielectric boundaries: the longitudinally magnetized case J. Phys. D: Appl. Phys. 11 1157–66

[15] Hlawiczka P 1978 The gyrotropic waveguide with a normal applied DC field J. Phys. D: Appl. Phys. 11 1941–8.

[16] I. Abdulhalim, Opt. Commun. 163, 9(1999) .

[17] C.X. Lian, X.Y. Li, J. Liu, Semicond. Sci. Technol. 19, 417 (2004) .

[18] J.J. Stamnes, D. Jiang, Opt. Commun. 150, 251 (1998).

[19] A. Mandatori, C. Sibilia, M. Bertolotti, S. Zhukovsky, J.W. Haus, M. Scalora, Phys. Rev. B 70, 165107 (2004)

[20] I. Abdulhalim, Opt. Commun. 215, 225 (2003).

[21] I. Abdulhalim, Opt. Commun. 157, 265 (1998).

[22] E. Cojocaru, Appl. Opt. 39 (34), 6441 (2000).

[23] A. Figotin, I. Vitebskiy, Phys. Rev. E 68, 036609 (2003).
[24] J. Lekner, J. Opt. Soc. Am. A 16, 2763 (1999).
[25] R. Yu, B.F. Zhu, Q.M. Wang, J. Phys. Condens. Matter 13, L559 (2001).
[26] A. Ciattoni, C. Palma, J. Opt. Soc. Am. A 20, 2163 (2003).
[27] C. Gu, P. Yeh, J. Opt. Soc. Am. A 10, 966 (1993).
[28] J.J. Stamnes, G.S. Sithambaranathan, J. Opt. Soc. Am. A 18, 3119 (2001).
[29] G.V. Morozov, D.W.L. Sprung, J. Martorell, Phys. Rev. E 70, 016606 (2004).
[30] A. Figotin, I. Vitebskiy, Phys. Rev. E 67, 165210 (2003)
[31] D.W. Berreman, J. Opt. Soc. Am. A 62, 502 (1972).
[32] P. Yeh, Optical Waves in Layered Media, Wiley, New York, 1988 (Chapter 9).
[33] D. Bria, B. Djafari-Rouhani, E.H. El Boudouti, A. Mir, A. Akjouj, A. Nougaoui, J. Appl. Phys. 91, 2569 (2002)
[34] D. Bria, B. Djafari-Rouhani, A. Akjouj, L. Dobrzynski, J.P. Vigneron, E.H. El Boudouti, A. Nougaoui, Phys. Rev. E 69, 066613 (2004).
[35] M.L.H. Lahlaouti, A.Akjouj, B. Djafari-Rouhani, , L. Dobrzynski, M.Hammouchi, E.H. El Boudouti, A. Nougaoui, Phys. Rev.B, 63, 035312 (2001)
[36] L. Dobrzynski, Surf.Sci.180, 489 (1987), Surf. Sci.Rep.11,139(1990)
[37] L. Dobrzynski and H. Puszkarski, J. Phys, Condens. Mater5,139(1993).
[38] H. Goldstein, Classical Mechanics, Addison-Wesley, Reading, MA, 1957, pp. 107–109 (Chapter 4).
[39] G.D. Landry, T.A. Maldonado, J. Opt. Soc. Am. A 12, 2048 (1995).
[40] N. Ouchani, D. Bria, A. Nougaoui, B. Djafari-Rouhani, Solar cells 90 (2006) 1445-1457.

Appendix

1- The bulk Green's function elements are given by:

$$
\begin{aligned}
G_{XX}\left(Z,Z'\right)&=-\frac{C}{2\alpha_+\alpha_-}\left[\alpha_- A_- e^{-\alpha_+|Z-Z'|}-\alpha_+ A_+ e^{-\alpha_-|Z-Z'|}\right]\\
G_{YX}\left(Z,Z'\right)&=-\frac{B}{D}\frac{C}{2\alpha_+\alpha_-}\left[\alpha_- e^{-\alpha_+|Z-Z'|}-\alpha_+ e^{-\alpha_-|Z-Z'|}\right]\\
G_{ZX}\left(Z,Z'\right)&=-\frac{iq_yC}{2}\frac{\varepsilon_{XY}}{\varepsilon_{ZZ}}\left[e^{-\alpha_+|Z-Z'|}-e^{-\alpha_-|Z-Z'|}\right]\mathrm{sgn}\left(Z-Z'\right)\\
G_{XY}\left(Z,Z'\right)&=-\frac{B}{D}\frac{C}{2\alpha_+\alpha_-}\left[\alpha_- e^{-\alpha_+|Z-Z'|}-\alpha_+ e^{-\alpha_-|Z-Z'|}\right]\\
G_{YY}\left(Z,Z'\right)&=-\frac{C}{2\alpha_+\alpha_- D}\left[\alpha_- A_+ e^{-\alpha_+|Z-Z'|}-\alpha_+ A_- e^{-\alpha_-|Z-Z'|}\right]\\
G_{ZY}\left(Z,Z'\right)&=-\frac{C}{2}\frac{iq_Y}{q_0^2\varepsilon_{ZZ}}\left[A_+ e^{-\alpha_+|Z-Z'|}-A_- e^{-\alpha_-|Z-Z'|}\right]\mathrm{sgn}\left(Z-Z'\right)\\
G_{XZ}\left(Z,Z'\right)&=-\frac{iq_yC}{2}\frac{\varepsilon_{XY}}{\varepsilon_{ZZ}}\left[e^{-\alpha_+|Z-Z'|}-e^{-\alpha_-|Z-Z'|}\right]\mathrm{sgn}\left(Z-Z'\right)\\
G_{YZ}\left(Z,Z'\right)&=-\frac{C}{2}\frac{iq_Y}{q_0^2\varepsilon_{ZZ}}\left[A_+ e^{-\alpha_+|Z-Z'|}-A_- e^{-\alpha_-|Z-Z'|}\right]\mathrm{sgn}\left(Z-Z'\right)\\
G_{ZZ}\left(Z,Z'\right)&=\frac{1}{\left(q_Y^2-q_0^2\varepsilon_{ZZ}\right)}\left[\frac{1}{D}\delta\left(Z-Z'\right)+\frac{C}{2}\frac{q_Y^2}{q_0^2\varepsilon_{ZZ}}\left(\alpha_+ A_+ e^{-\alpha_+|Z-Z'|}-\alpha_- A_- e^{-\alpha_-|Z-Z'|}\right)\right]
\end{aligned}
\tag{9}
$$

where:

$A_\pm=(q_Y^2-q_0^2\,\varepsilon_{XX}-\alpha_\pm^2)$, $B=q_0^2\,\varepsilon_{XY}$, $C=\left(\alpha_+^2-\alpha_-^2\right)^{-1}$, $D=q_0^2\varepsilon_{ZZ}\left(q_Y^2-q_0^2\,\varepsilon_{ZZ}\right)$ and $\delta(Z-Z')$ the Dirac delta function.

$q_0=\dfrac{\omega}{c}$ is the vacuum wave vector, c is the velocity of light in vacuum and ω is the frequency of optical wave.

ε is the dielectric tensor defined in the laboratory system in the laboratory system (XYZ), with $\theta=0$, $\psi=0$ and an arbitrary value of the azimuth angle ϕ, by:

$$
\vec{\varepsilon}=\begin{pmatrix}
\varepsilon_x\cos^2(\phi)+\varepsilon_y\sin^2(\phi) & (\varepsilon_x-\varepsilon_y)\sin(\phi)\cos(\phi) & 0\\
(\varepsilon_x-\varepsilon_y)\sin(\phi)\cos(\phi) & \varepsilon_x\sin^2(\phi)+\varepsilon_y\cos^2(\phi) & 0\\
0 & 0 & \varepsilon_z
\end{pmatrix}
\tag{10}
$$

$\alpha_\pm$ are defined as:

$$
-q_Z{}^2=\alpha_\pm{}^2=\frac{1}{2\varepsilon_{ZZ}}\left\{\begin{array}{l}
\left[q_y{}^2\left(\varepsilon_{ZZ}+\varepsilon_{YY}\right)-q_0{}^2\varepsilon_{ZZ}\left(\varepsilon_{XX}+\varepsilon_{YY}\right)\right]\\
\pm\left[\left[k_Z{}^2\varepsilon_{YY}-\varepsilon_{ZZ}\left(q_Y{}^2-q_0{}^2\varepsilon_{XX}\right)\right]^2-4\,q_0^2\,k_Z{}^2\,\varepsilon_{ZZ}\,\varepsilon_{XY}{}^2\right]^{\frac{1}{2}}
\end{array}\right\}
\tag{11}
$$

where $k_Z{}^2=q_Y{}^2-q_0{}^2\varepsilon_{ZZ}$.

2- The surface element matrix of an homogenous medium i with free surface:

$$
\vec{g}_i\left(MM\right)^{-1}=\begin{pmatrix}
\vec{\vec{A}}_i & \vec{\vec{B}}_i\\
\vec{\vec{B}}_i & \vec{\vec{A}}_i
\end{pmatrix}
\tag{12}
$$

where $\vec{\vec{A}}_i$ *and* $\vec{\vec{B}}_i$ are 2×2 matrixes, whose elements are the forms:

$$\vec{\vec{A}}_i = \begin{pmatrix} r_i & q_i \\ q_i & k_i \end{pmatrix} \qquad and \quad \vec{\vec{B}}_i = \begin{pmatrix} h_i & f_i \\ f_i & e_i \end{pmatrix} \tag{13}$$

where r_i, q_i, k_i, h_i, f_i and e_i are defined as:

$$\begin{aligned}
r_i &= -C_i \left[\alpha_{i+} A_{i-} \coth\theta_{i+} - \alpha_{i-} A_{i+} \coth\theta_{i-}\right] \\
q_i &= C_i B_i \left[\alpha_{i+} \coth\theta_{i+} - \alpha_{i-} \coth\theta_{i-}\right] \\
k_i &= -C_i D_i \left[\alpha_{i+} A_{i+} \coth\theta_{i+} - \alpha_{i-} A_{i-} \coth\theta_{i-}\right] \\
h_i &= C_i \left[\alpha_{i+} A_{i-} \left(sh\theta_{i+}\right)^{-1} - \alpha_{i-} A_{i+} \left(sh\theta_{i-}\right)^{-1}\right] \\
f_i &= C_i B_i \left[\alpha_{i-} \left(sh\theta_{i-}\right)^{-1} - \alpha_{i+} \left(sh\theta_{i+}\right)^{-1}\right] \\
e_i &= -C_i D_i \left[\alpha_{i-} A_{i-} \left(sh\theta_{i-}\right)^{-1} - \alpha_{i+} A_{i+} \left(sh\theta_{i+}\right)^{-1}\right]
\end{aligned} \tag{14}$$

with:

$$A_{i\pm} = (q_Y^2 - q_0^2\, \varepsilon_{XX}^{(i)} - \alpha_{i\pm}^2),\ B_i = q_0^2\, \varepsilon_{XY}^{(i)},\ C_i = \left(\alpha_{i+}^2 - \alpha_{i-}^2\right)^{-1},\ D_i = q_0^2 \varepsilon_{ZZ}^{(i)} \left(q_Y^2 - q_0^2\, \varepsilon_{ZZ}^{(i)}\right)$$

3- The expressions of the amplitude transmitted (t_{SS}, t_{PS}) and reflected (r_{SS}, r_{PS}) coefficients, when a pure (S) waves is incident, are the form:

$$\begin{aligned}
r_{SS} &= -(2\alpha d_{11} + 1) \\
r_{PS} &= -(2\alpha d_{21}) \frac{B_S}{B_P} \\
t_{SS} &= -(2\alpha d_{13}) \\
t_{PS} &= -(2\alpha d_{23}) \frac{B_S}{B_P}
\end{aligned} \tag{15}$$

where $\alpha = (k_{//}^2 - \frac{\omega^2 \varepsilon_S}{c^2})^{\frac{1}{2}}$, $k_{//}$ is the wave vector parallel to the (XY) interfaces, ω is the frequency of optical wave, c the speed of light in vacuum and ε_S the permittivity of substrate.

B_S=1 is the amplitude of the S-input wave and B_P ($B_P = \frac{-i\alpha c}{\omega\sqrt{\varepsilon_S}}$) is the amplitude of the P-input wave.

d_{11}, d_{21}, d_{13}, d_{23} are the elements of tranked matrix of the finite system presented in figure 1.

4- The expressions of the amplitude transmitted (t_{PP}, t_{SP}) and reflected (r_{PP}, r_{SP}) coefficients, when a pure TM (P) waves is incident, are of the form

$$
\begin{aligned}
r_{PP} &= (\frac{2q_0^2\varepsilon_S}{\alpha} d_{22} - 1) \\
r_{SP} &= (\frac{2q_0^2\varepsilon_S}{\alpha} d_{12}) \frac{B_P}{B_S} \\
t_{SP} &= (\frac{2q_0^2\varepsilon_S}{\alpha} d_{14}) \frac{B_P}{B_S} \\
t_{PP} &= (\frac{2q_0^2\varepsilon_S}{\alpha} d_{24})
\end{aligned}
\tag{16}
$$

the same as, d_{12}, d_{22}, d_{14}, d_{24} are the element of tranked matrix of the finite system.

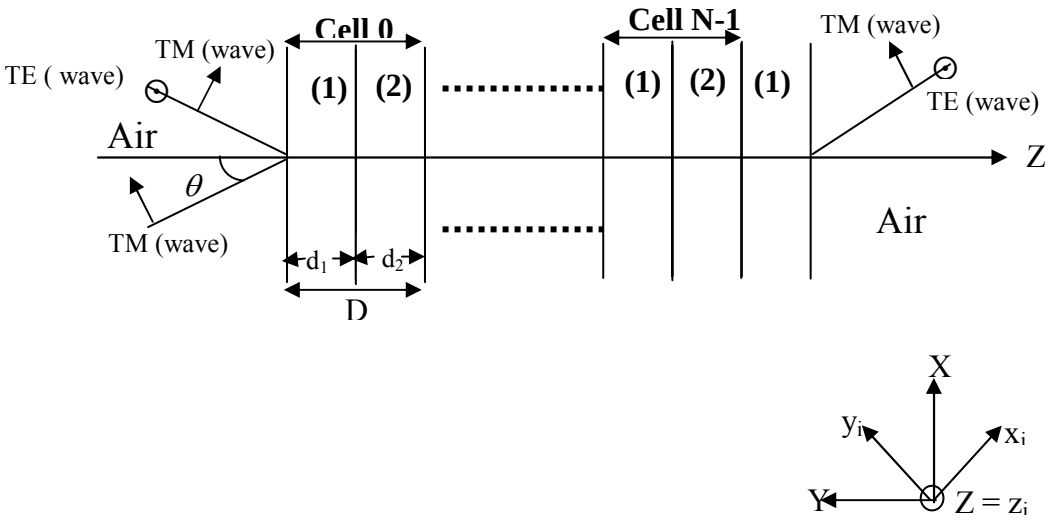

Figure 1: Anisotropic multilayers structure, formed by two birefringent biaxial layers: N+1 layers of $NaNO_2$ and N layers of SbSI, d_i (i=1,2) is the thickness of layer i, D is the period of the finite system, and θ is the incident angle with respect to the z-axis. The crystal of the first layer has the principal axis directed along the direction of Cartesian axis while the crystal of the second layer is rotated with respect to the first one by the azimuth angle ϕ around the z axis. The input and output isotropic medium is air.

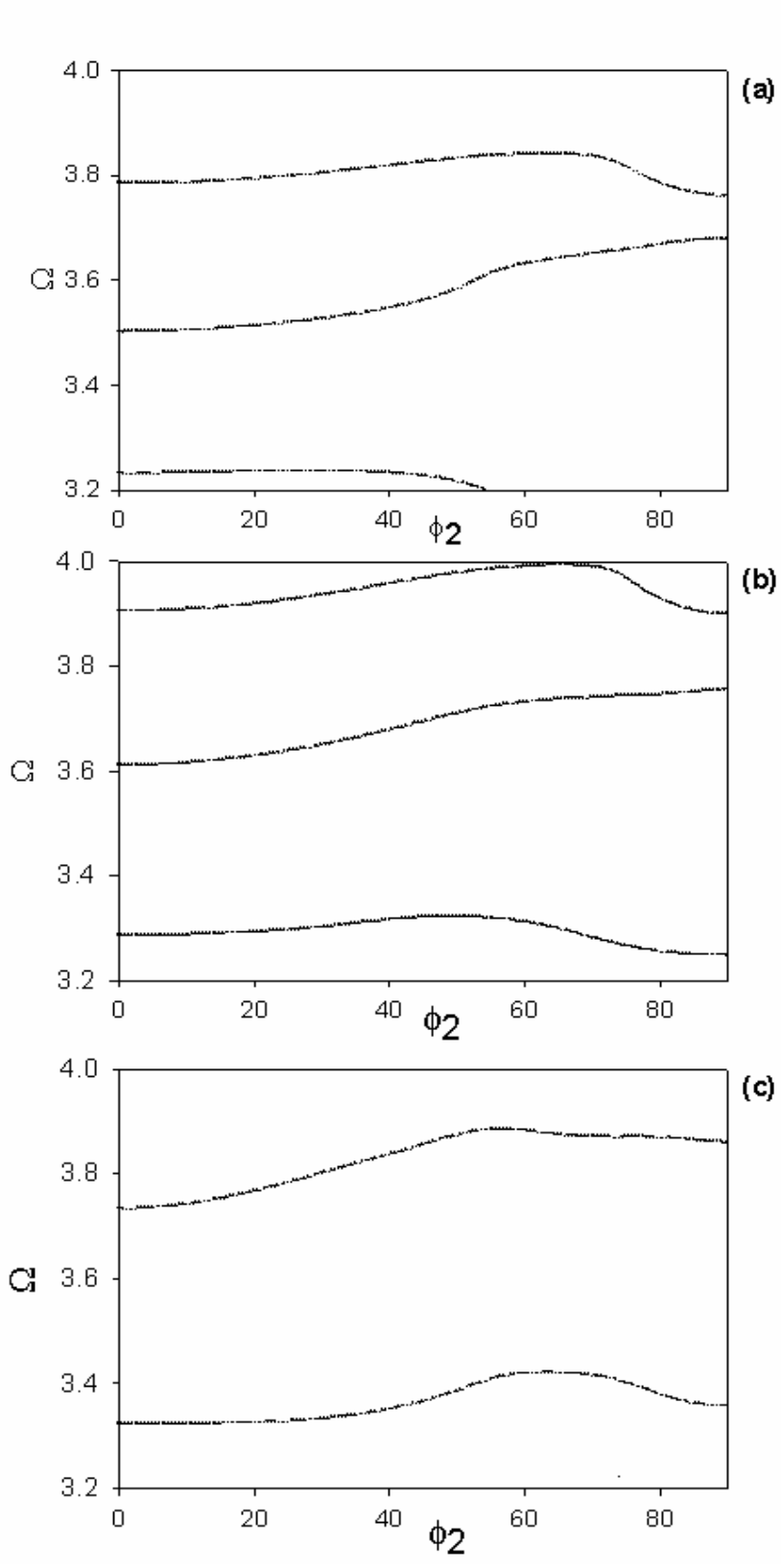

Figure 2: Reduced frequency $\Omega\,(\Omega = \frac{\omega D}{2\pi})$ as a function of azimuthal angle of the SbSI layers, for several values of the incidence angle: $(a)\theta = 0°, (b)\theta = 30° \; and \; (c)\theta = 45°$. The input wave is of P polarization.

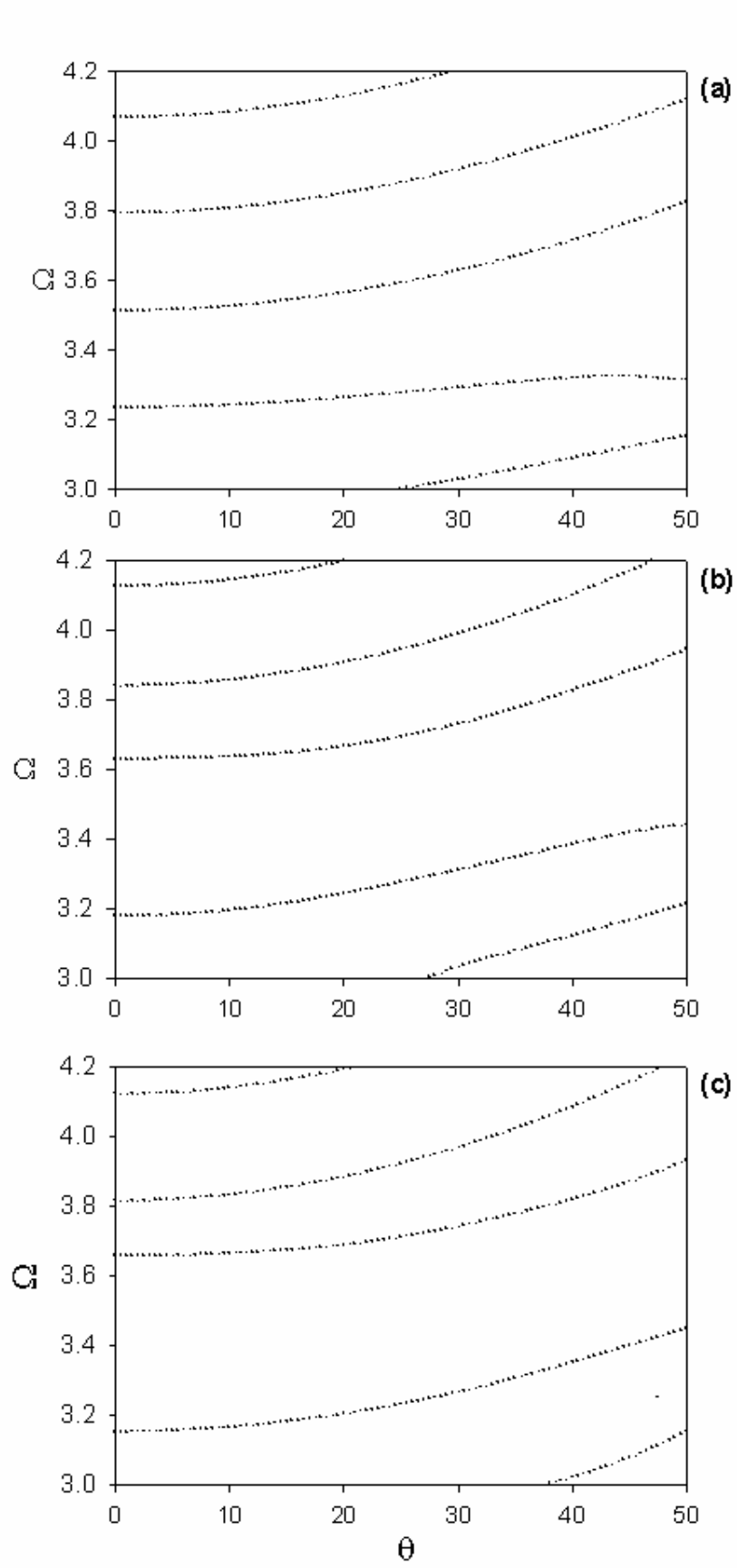

Figure 3: Variation of the reduced frequency **Ω** as a function of the incidence angle θ, for $(a)\,\phi_2 = 20°, (b)\,\phi_2 = 60°\ and\ (c)\,\phi_2 = 75°$. The incident wave is P polarized.

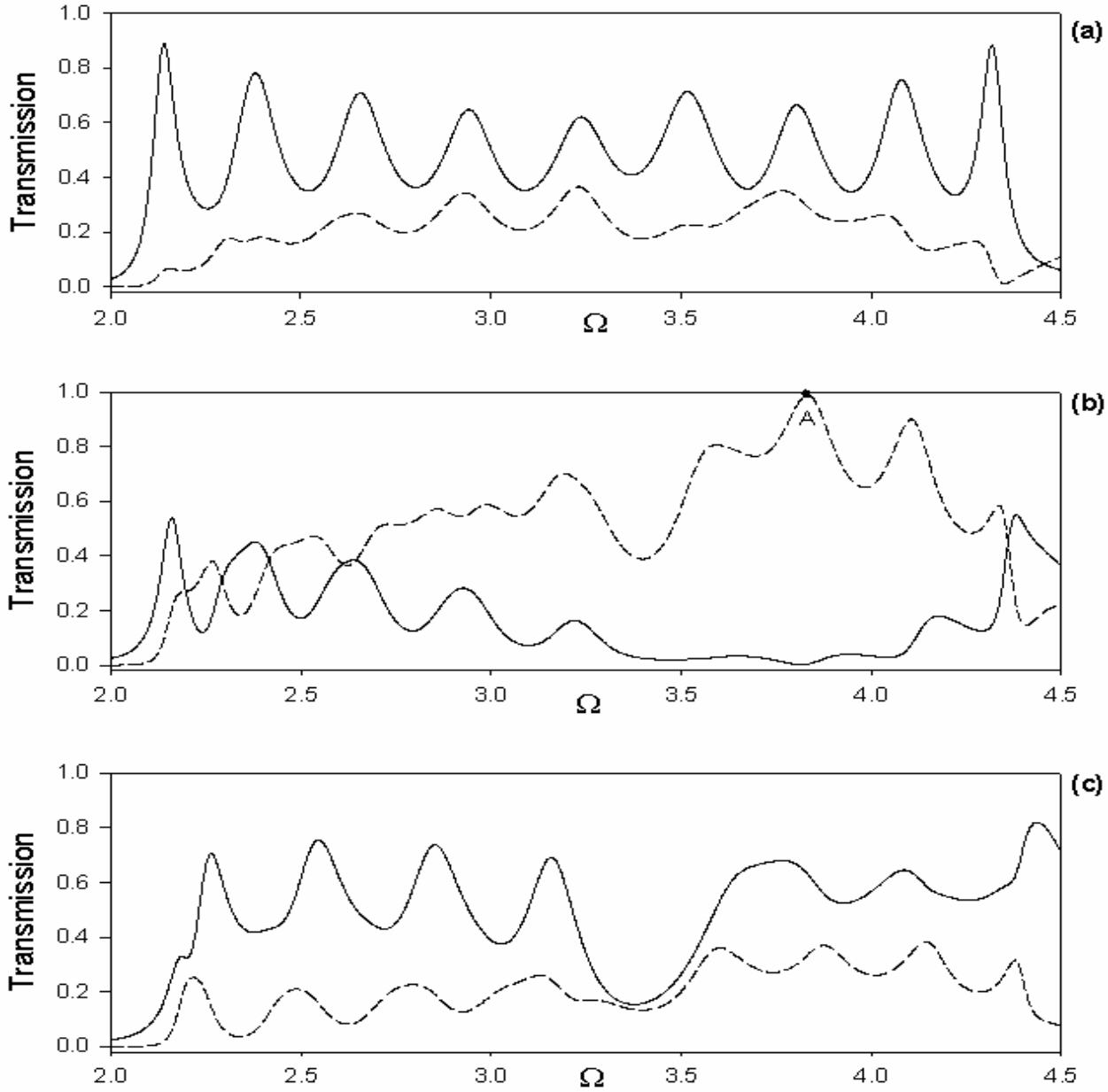

Figure 4: transmission coefficients as function of the reduced frequency Ω at normal incidence and for several values of the azimuth angle of the SbSI layers, namely $(a)\,\phi_2 = 25°, (b)\,\phi_2 = 53°\ and\ (c)\,\phi_2 = 75°$ while keeping $\phi_1 = 0°$. The solid and the short-dash lines represent respectively the T_{PP} and T_{SP} transmission coefficients. The incoming light has a transverse magnetic polarization.

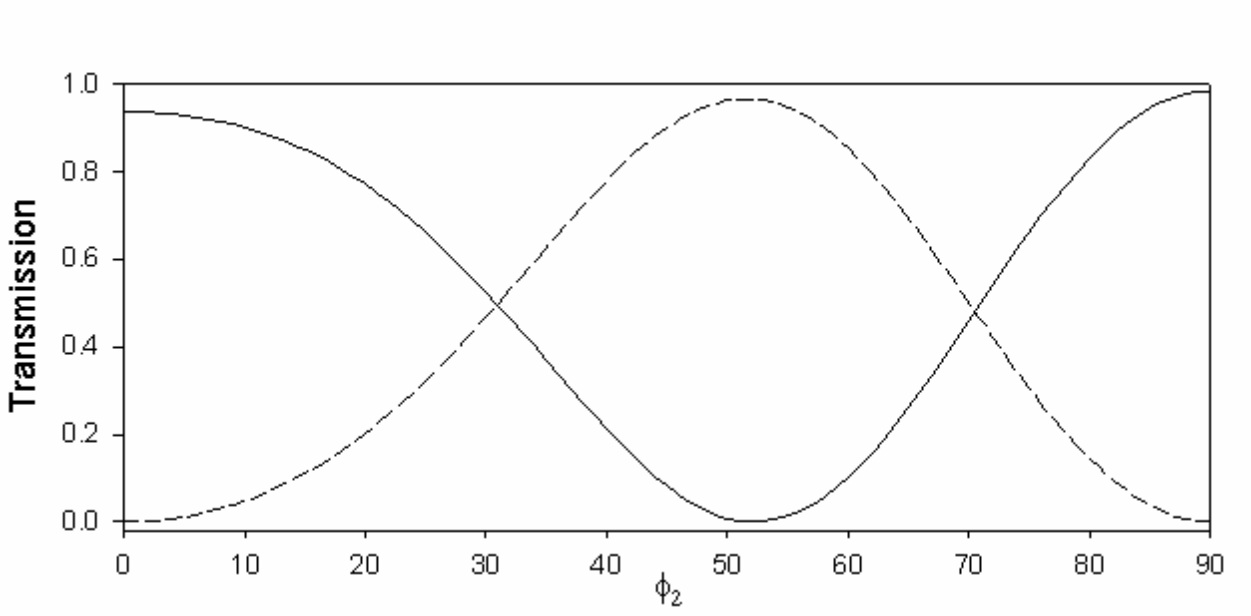

Figure 5: Transmission coefficients as function of the azimuth angle ϕ_2 of SbSI at the point A shown in figure (4-b). The solid and the short-dash lines have the same meaning as in figure 4.

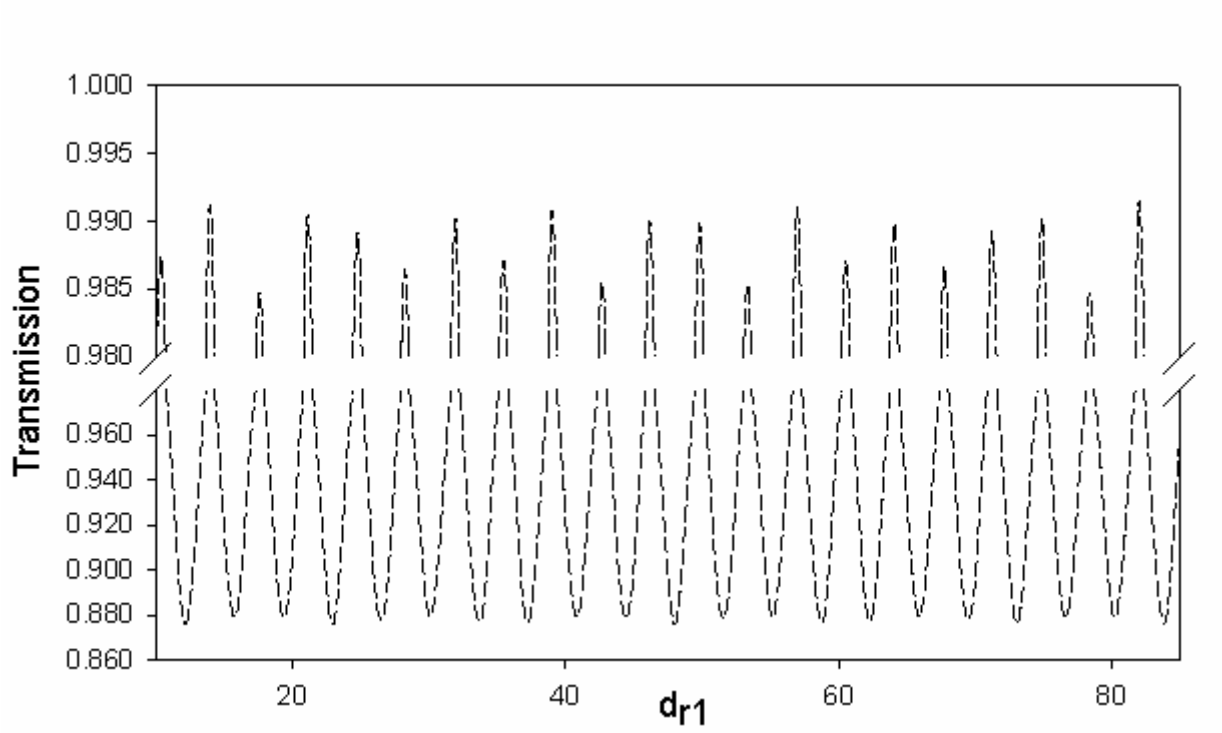

Figure 6: Variation of converted wave transmission versus the thickness d_{r1} of medium 1 in cell (N+1) with d_{l1} =2.01D, the thickness of the first layer for the SL depicted in figure1.

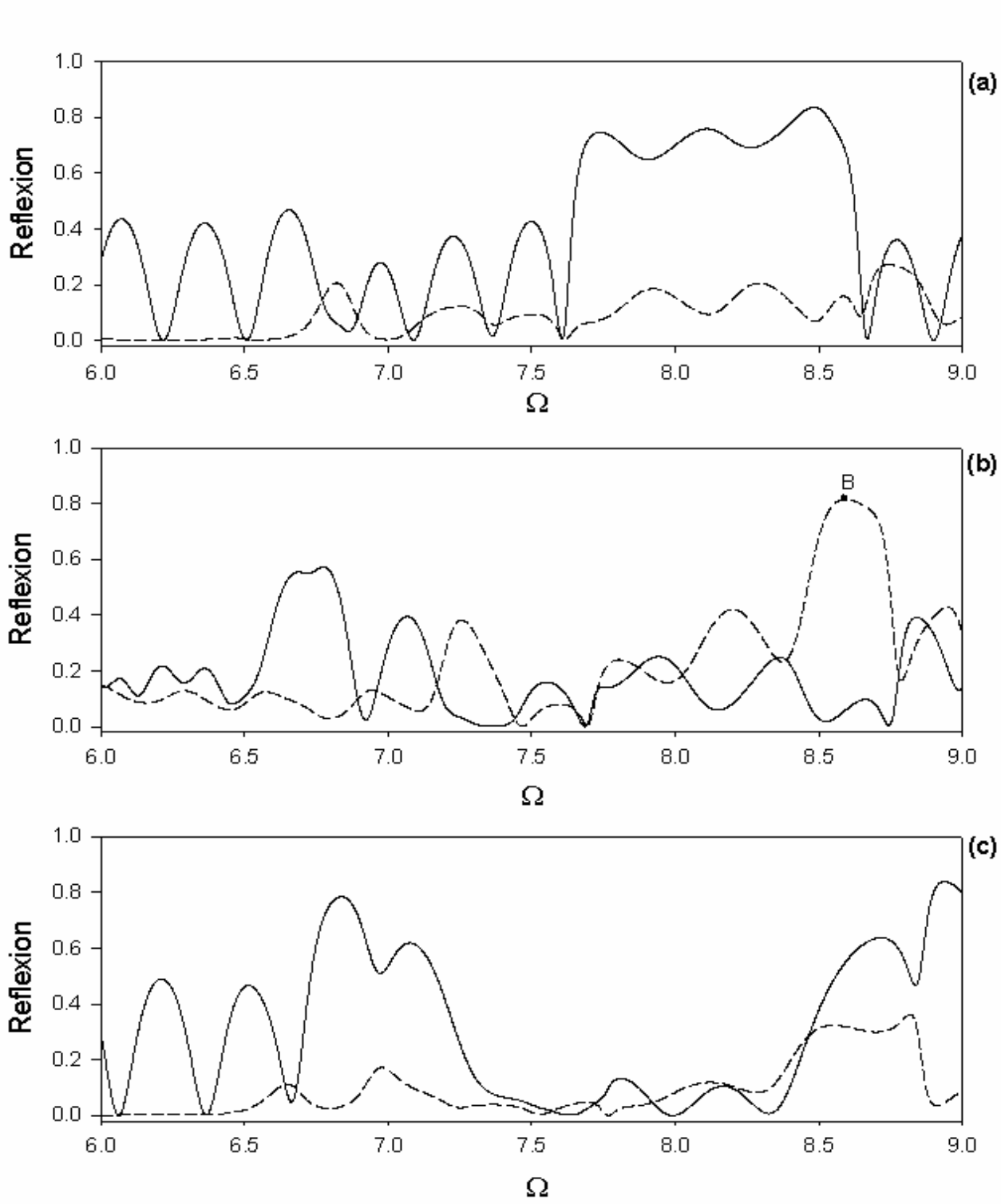

Figure 7: Variation of the reflection coefficients as a function of the reduced frequency Ω when incident angle is 15° with respect to the z axis for $(a)\,\phi_2 = 25°, (b)\,\phi_2 = 54°\ and\ (c)\,\phi_2 = 75°$. The solid and the short-dash lines represent respectively the R_{PP} and R_{SP} reflection coefficients. The incident light has a transverse-magnetic polarization.

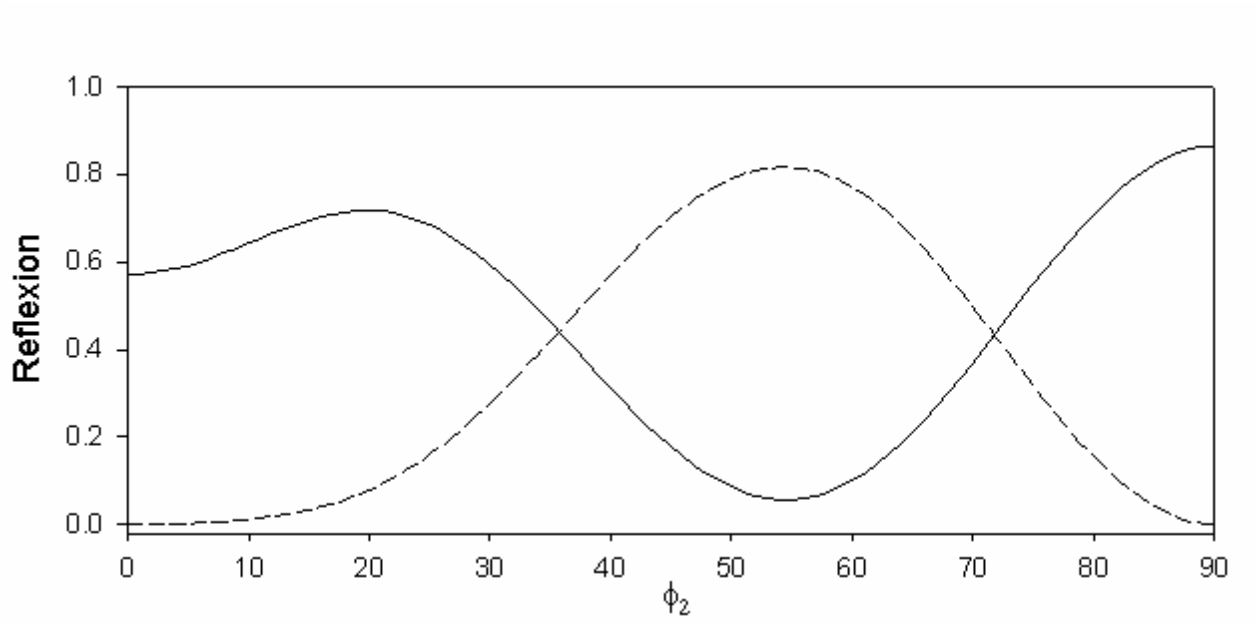

Figure 8: reflection coefficients as function of the azimuth angle ϕ_2 of SbSI at the point B shown in Fig (7-b). The solid and the short-dash lines have the same meaning as in Fig7.

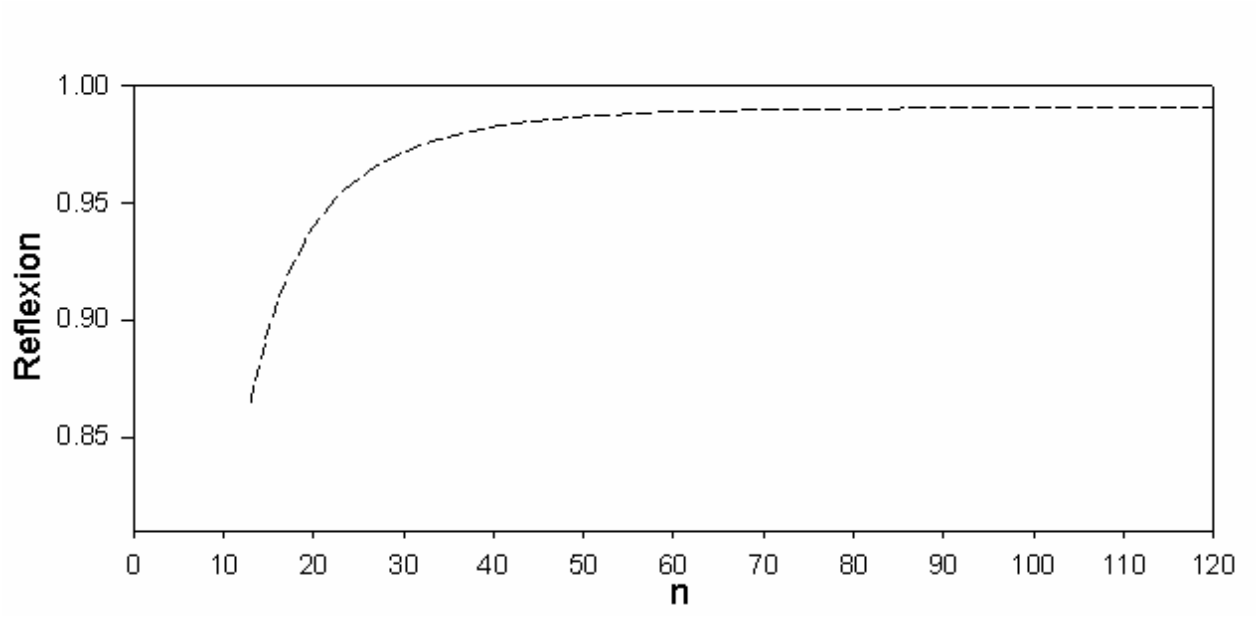

Figure 9: Variation of the amplitude of the converted wave versus the total number of layers n=2N+1 of the system presented in Fig1.